DOI: https://doi.org/10.54966/jreen.v29i4.1786

Journal of Renewable Energies

Revue des Energies Renouvelables

Journal home page: https://revue.cder.dz/index.php/rer

Conference paper

Techno-economic and environmental optimisation of photovoltaic systems based on self-consumption with surplus grid injection for industrial buildings

Fatiha Smain [a,*]

[a] *Theoretical Physics Laboratory, Department of Physics, Abou Bekr Belkaid University, 13000, Tlemcen, Algeria*

ARTICLE INFO

Article history:
Received February 26, 2026
Revised June 30, 2026
Accepted June 30, 2026
Available online July 1, 2026
Published July 14, 2026

Keywords:
Rooftop PV,
Industrial self-consumption,
Grid integration,
Multi-criteria approach,
Energy optimization.

ABSTRACT

This study evaluates the technical, economic, and environmental feasibility of a rooftop photovoltaic system for an industrial facility consuming 67184 kWh/year. The system is optimised for self-consumption, with surplus exported to the grid. Modelling and PVsyst simulations considered the load profile, rooftop geometry and corrected solar irradiation. Four Photovoltaic capacities (30, 40, 50, and 60 kWp) were analysed. A multi-criteria approach was applied to assess their performance across technical, economic, and environmental pillars. The 30 kWp system is undersised, while the 60 kWp system produces excessive surplus. Compared to the 40 kWp system, the 50 kWp configuration generates 26 % more energy, 23.8 % more surplus, and requires 15 % higher capital expenditure. The 40 kWp system delivers 49807 kWh/year, of which 25702 kWh are self-consumed, with an 8-year payback. CO_2 emissions avoided reach 285.6 t over 25 years, with a 5-year carbon payback. The multi-criteria analysis identifies the 40 kWp system as the optimal solution.

1. INTRODUCTION

The transition towards a sustainable energy model with low greenhouse gas emissions is essential to mitigate climate change. Renewable energy sources, and particularly solar photovoltaic (PV) energy, play a central role in this transition. By the end of 2024, the global installed PV capacity exceeded 2.2 TW, with nearly 600 GW of new installations expected in 2025 (Jäger Waldau, 2025). In parallel, the industrial sector accounts for approximately 37% of global electricity consumption (IEA, 2025), making

* *Corresponding author, E-mail address: fatiha.smain@univ-tlemcen.dz*

ISSN: 1112-2242 / EISSN: 2716-8247

This work is licensed under a Creative Commons Attribution-ShareAlike 4.0 International License CC-BY-NC-SA

Selection and peer-review under responsibility of the Technical Committee of the International Conference on Fossil and Renewable Energies (ICFRE 2025)

it a priority area for PV integration. Self-consumption systems with surplus electricity injection help reduce energy costs, decentralise electricity production, and lower the carbon footprint, while enabling the utilisation of excess generation. However, rigorous planning is required to match solar production with the variability of industrial load profiles and to avoid technical or financial imbalances.

Recent studies have highlighted the importance of appropriate system sizing to maximise the performance of industrial PV installations, particularly by reducing losses associated with mismatches between generation and consumption. Sánchez-Jiménez et al. (2025) evaluated self-consumption PV systems on industrial rooftops in a continental Mediterranean climate, demonstrating the influence of multi-string topology on usable energy production and economic performance. García et al. (2023) analysed profitability and optimal sizing in the agri-food industry, accounting for seasonality and electricity price fluctuations. Rouabhia et al. (2025) developed a real-time monitoring system for rapid fault detection and consumption analysis. Başaran et al. (2025) evaluated the optimal sizing and economic performance of an industrial photovoltaic (PV) system coupled with energy storage, drawing on real-world operational data. The assessment relied on standard financial metrics, including net present value (NPV) and payback period, to quantify project viability. Hu et al. (2020) examined the integration of thin-film PV modules on lightweight steel industrial roofs. Their study employed a comprehensive life-cycle cost–benefit analysis that accounted for both economic returns and environmental impacts.

Although industrial photovoltaic systems have been widely investigated, only a limited number of studies adopt a truly integrated framework that simultaneously addresses technical sizing, economic performance, and environmental impact. Structured methodologies capable of systematically comparing multiple installed capacities—and identifying an optimal configuration with respect to self-consumption rate, surplus export, financial returns, and life-cycle CO_2 emissions—remain scarce. This methodological gap constrains evidence-based decision-making and complicates the accurate sizing and optimisation of self-consumption PV systems in industrial buildings.

This study proposes an integrated framework for the sizing and evaluation of a grid-connected industrial photovoltaic system focused on self-consumption and surplus management. The approach combines technical, economic, and environmental analyses to assess the impact of system sizing on energy performance, profitability, and contribution to decarbonisation. The paper is organised as follows: Section 2 presents the methodology, Section 3 reports and discusses the results, and Section 4 concludes on the technical feasibility, economic viability, and environmental implications. The findings provide practical benchmarks for optimising industrial PV systems and promoting sustainable practices in the energy sector.

2. METHODOLOGY AND MATERIALS

2.1 Site location and industrial load profile

The photovoltaic installation is located on the rooftop of an industrial building in Ferrol, Spain, at coordinates 43°31′14.83″ N (latitude) and 8°11′12.37″ W (longitude). The building measures 65 m × 37 m, as shown in Figure 1 generated from Google Earth Pro. The available rooftop area totals 1,470 m², distributed across two roof slopes inclined at 6° and oriented toward the south-west and north-east, respectively. Access and maintenance walkways 1.5 m wide are provided, while seven skylights are excluded from the installation area. According to historical meteorological records from MeteoGalicia, the minimum ambient temperature at the site is −3 °C and the historical maximum temperature reaches 39.6 °C.

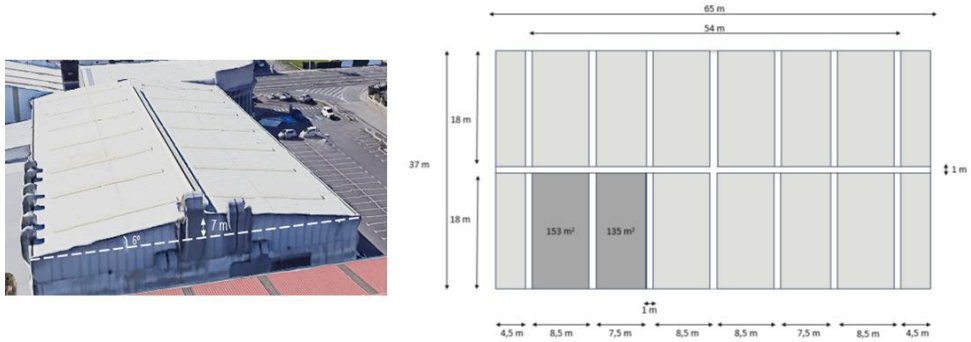

Fig 1. Rooftop configuration of the industrial building obtained from Google Earth Pro.

Figure 2 presents the factory's load profile, highlighting significant seasonal fluctuations. Industrial activity peaks in March, with an average daily demand of 261 kWh. Production slows during the summer months, reaching a minimum of 129 kWh/day in July. The total annual electricity consumption is estimated at 67184 kWh. These variations in demand constitute a critical factor for PV system sizing.

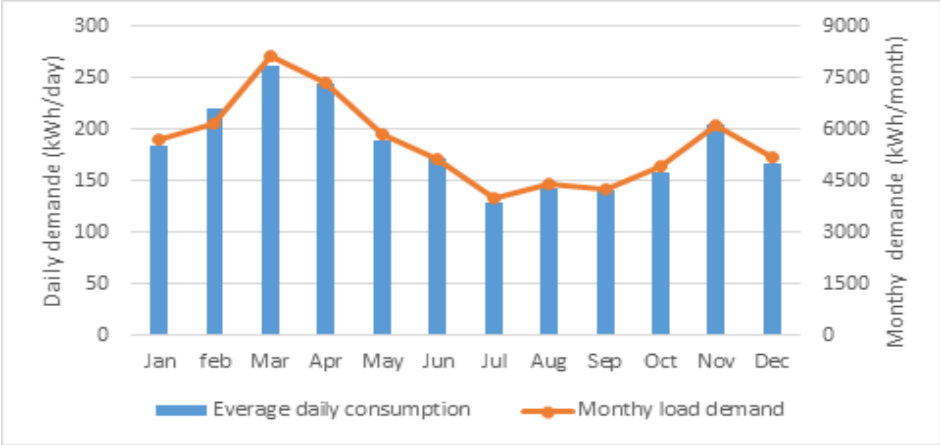

Fig 2. Evolution of the industrial load: average daily and monthly electricity consumption.

Given the variable industrial load, the photovoltaic system was sized using the self-consumption rate (SCR) as the main design criterion. The SCR is defined by Equation (1) as the ratio of locally generated photovoltaic energy directly consumed on-site E_{Load} to the total photovoltaic energy generated E_{PV} over a given period (Ciocia et al., 2021):

$$\mathrm{SCR} = \frac{E_{Load}}{E_{PV}} \tag{1}$$

In this study, the PV system was designed to achieve a target SCR of 40–60%. This range was selected to maximise on-site energy use while limiting grid exports and avoiding unnecessary PV system oversizing.

2.2 Technical study

The technical section presents the sizing and simulation methods for photovoltaic systems (Bouroumeid et al., 2024; Hazem et al., 2025; Yıldırım & Düzkaya, 2025; Zaghba et al., 2025).

2.2.1 Energy demand characterisation

The industrial unit's load profile was analysed at daily, monthly and annual scales to describe the temporal variability of consumption. This analysis enables the identification of the base load energy E_{Load} and the determination of the required peak power. The peak power of the photovoltaic generator P_{PV} is sized primarily to meet the base load demand, to optimise the self-consumption share and limit surplus electricity injected into the grid. For a given performance ratio (*PR*) and corrected solar irradiation G, the peak power is calculated using Equation (2) (Kalogirou, 2017) :

$$P_{PV} = \frac{E_{Load}}{\left(\frac{G}{G_{STC}}\right) x\ PR} \tag{2}$$

where G_{STC} is the reference solar irradiance under Standard Test Conditions (STC), equal to 1 kW/m². This study employs detailed technical modelling to deliver a preliminary pre-feasibility assessment and a decision-support framework for PV system sizing and optimisation.

2.2.2 Corrected solar irradiation

Corrected solar irradiation was estimated from data provided by the PVGIS tool. Module orientation was defined according to the azimuth of the roof slope, evaluated using the software Suncalc. Corrected solar irradiation was evaluated for two module-tilt configurations (β):

- Tilt imposed by the geometry of the existing roof, equivalent to 6°,
- Annual optimal tilt β_{opt}, calculated using an empirical relationship given by Equation (3), as a function of the site latitude ∅ (Kalogirou, 2017).

$$\beta_{opt} = 3.7 + (0.69x\ \emptyset) \tag{3}$$

The selected configuration corresponds to the one that maximises energy performance at the lowest cost.

2.2.3 Equipment selection and PV system configuration

The photovoltaic modules and inverter were selected to ensure electrical compatibility and system reliability over the entire lifecycle, estimated at 25 years. The electrical parameters of the modules under standard test conditions (open-circuit voltage V_{OC} , short-circuit current I_{SC} and maximum power point P_{MPP}) were corrected to account for actual operating conditions (Belhaouas et al., 2025). These adjustments were performed using Equations (4), (5) and (6) (Kalogirou, 2017).

$$V_{OC}(T_m) \cong V_{OC}[1 + k_{Voc} * (T_m - 25)] \tag{4}$$

$$I_{SC}(T_m) = I_{SC}[1 + k_{ISc} * (T_m - 25)] \tag{5}$$

$$P_{MPP}(T_m) = P_{MPP}[1 + k_{Pot} * (T_m - 25)] \tag{6}$$

where T_m denotes the module temperature, k_{Voc}, k_{ISc} and k_{Pot} are the module temperature correction coefficients for open-circuit voltage, short-circuit current and maximum power, respectively.

The total number of modules (N_{mod}) is obtained by dividing the target peak power (P_{peak}) by the rated power of a single module (P_{mod}). To identify the adequate PV system peak power, several peak power configurations were tested. The energy yield of each configuration was compared with the factory consumption profile. The selected configuration is the one that maximises the match between generation and demand. This step defines the optimal size of the photovoltaic array. The number of modules connected in series (N_S) is chosen to comply with the inverter voltage limits. Consequently, the number of series modules must satisfy the inequality given by Equation (7):

$$N_{S,min} \leq N_S \leq N_{S,max} \quad , \quad N_{S,min} = \frac{V_{Ond,min}}{V_{MPPT,max}} \quad , \quad N_{S,max} = \frac{V_{Ond,max}}{V_{MPPT,min}} \tag{7}$$

where $V_{inv,min}$ and $V_{inv,max}$ denote the minimum and maximum inverter voltages, respectively. $V_{MPPT,min}$ and $V_{MPPT,max}$ are the minimum and maximum module voltages within the MPPT operating range. The number of parallel strings (N_{string}) is determined by the ratio between the inverter's maximum allowable current and the modules short-circuit current, as expressed in Equation (8).

$$N_{string} = I_{Inv,max}/I_{sc,max} \tag{8}$$

2.2.4 PVsyst simulation

The performance of the photovoltaic system was evaluated using PVsyst software (Laksono et al., 2025; PVsyst SA, 2024). Input data include: site-specific climatic conditions extracted from the Meteonorm database (irradiation, temperature, typical meteorological year), the analytically calculated module orientation and tilt, and the technical specifications of the modules and inverter (efficiency, voltages, currents and rated power). The simulation quantifies energy production, energy injected into the grid and energy losses. These results are used to validate the electrical sizing and to optimise the PV system configuration.

2.3 Economic study

The economic analysis is based on the calculation of the total investment cost (C_{inv}) and the determination of the payback period (PBP) (Camilo et al., 2017; Mohand Kaci et al., 2024; Pedrero et al., 2021). The investment cost is calculated using Equation (9) and encompasses the costs of components and labour (C_{lab}). The parameters $P_{i,unit}$ and Q_i are the unit price and the quantity of the component (i) respectively.

$$C_{inv} = \sum_i \left(P_{i,unit} x Q_i\right) + C_{lab} \tag{9}$$

The net annual revenue (R_{an}), is calculated using Equation (10). It represents the sum of savings resulting from self-consumption and revenues generated by the sale of surplus electricity.

$$R_{an} = \left(E_{sc} x P_{grid}\right) + \left(E_{inj} x P_{sell}\right) \tag{10}$$

where E_{sc} and E_{inj} denote the self-consumed and injected energies, respectively. P_{grid} and P_{sell} correspond to the purchase and selling tariffs. Operating and maintenance costs (OPEX) are assumed to be 1.5% of CAPEX. The net annual profit is obtained by deducting OPEX from the net annual revenue.

The payback period (PBP) is defined as the year n in which the cumulative cash flows offset the initial investment. It is calculated using Equation (11):

$$PBP = min\left\{n \mid \sum_{k=1}^{n} R_{an,k} \geq C_{inv}\right\} \quad (11)$$

2.4 Environmental assessment: Life Cycle Carbon balance of the PV installation

The environmental impact of the photovoltaic system is quantified by the Life Cycle Carbon emissions (LCE) over 25 years, following a cradle-to-grave approach (Neumüller et al., 2023; Rus et al., 2024). The embodied emissions (L_{emb}) correspond to the CO_2 emissions associated with the manufacture of the modules and inverter, transportation, installation and ancillary equipment, expressed in tonnes of CO_2 . The annual avoided emissions ($L_{avo,t}$) are calculated from the annual electrical production simulated with PVsyst, according to Equation (12):

$$L_{avo,t} = E_{avo,t}\ x\ EF_{grid} \quad (12)$$

where $E_{avo,t}$(kWh) is the energy produced in year and $EF_{grid} = 287$ gCO_2/kWh is the average grid emission factor adopted for the operational phase. The cumulative avoided emissions over 25 years are obtained using Equation (13):

$$L_{avo,tot} = t\sum_{t=1}^{25} L_{avo,t} \quad (13)$$

The cumulative carbon balance at year t is defined by Equation (14).

$$L_{net}(t) = \sum_{k=1}^{t} L_{avod,k} \quad (14)$$

2.5 Multi-criteria decision-making approach

Sizing photovoltaic (PV) systems requires decision-making that simultaneously considers diverse criteria, encompassing technical, economic, and environmental dimensions. Multi-criteria approaches offer a robust framework for integrating these objectives (Al Shumrani et al., 2026; Chen Jong & Mohamud Ahmed, 2024; Sánchez Jiménez et al., 2025).

In this study, the selection of the optimal PV configuration is based on a multi-criteria analysis structured around three complementary pillars: technical, economic, and environmental. Four peak power scenarios were simulated under identical assumptions, including the factory load profile and climatic conditions. For each scenario, three performance indicators were calculated and subsequently normalised to the interval [0, 1], enabling a dimensionless comparison. The solar fraction (FR) quantifies the alignment between PV generation and electricity consumption; the specific gain (€/kWp/year) assesses economic efficiency independently of system size, and the specific CO_2 avoided (tCO_2 /kWp/year) measures the environmental benefit per unit of installed capacity. The normalised indicators were compared graphically to identify the configuration that achieves the best balance across the three pillars of sustainable development. When two scenarios exhibit comparable performance, an

economic rationality criterion is applied, selecting the configuration with the lowest CAPEX to minimise the initial investment.

3. RESULTS AND DISCUSSIONS

3.1 Corrected tilted solar irradiation and PV system configuration

The geometric analysis conducted using the tool SunCalc determined an azimuth of 192.93° (true north), corresponding to a south-west orientation of 13°. The annual optimal tilt is estimated at θ = 30°, (Eq. 1). Figure 3 shows the variation of the average daily corrected irradiation for an installed capacity of 1 kWp, for two configurations: the configuration optimised on an annual basis (13°, 30°) and the coplanar configuration imposed by the building constraints (13°, 6°). During summer, the differences in irradiation are negligible. In winter, the corrected irradiation for the (13°, 30°) configuration is higher, with a maximum discrepancy in February (0.71 kWh/m²) and a secondary peak in December (0.69 kWh/m²). However, the coplanar configuration (13°, 6°) is retained because it reduces structural constraints and wind load, while facilitating the architectural integration of the modules.

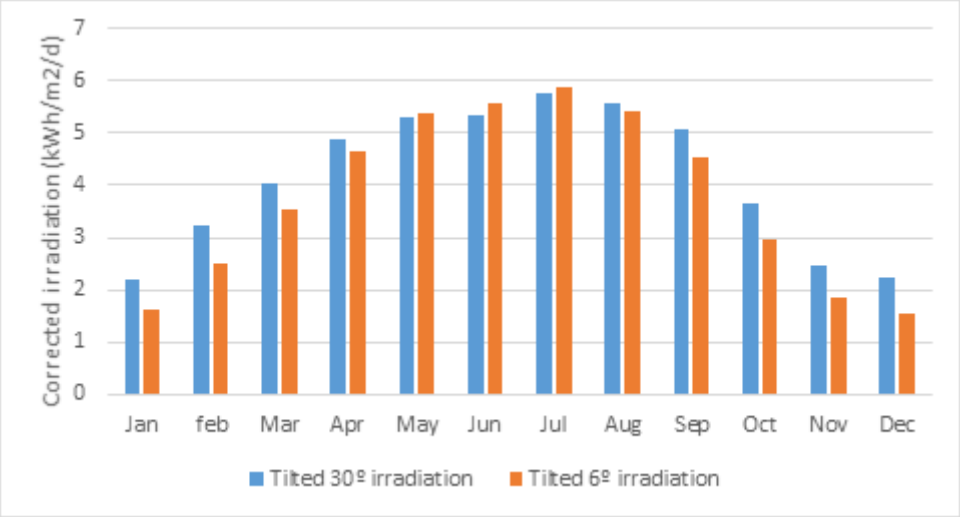

Fig 3. Average daily corrected irradiation (kWh/m²) for 1 kWp, comparing the optimal configuration (13°, 30°) with the roof configuration (13°, 6°).

To determine the optimal installed power for the industrial building, a sensitivity analysis was conducted. The annual production for four peak power levels (30, 40, 50 and 60 kWp) was simulated using PVsyst. Figure 4 shows the monthly demand (solid line) and the simulated PV production (dashed line) for each capacity scenario.

- **30 kWp:** PV production is insufficient to cover the base load. In March, 2192 kWh are produced compared with a demand of 8106 kWh.
- **40 kWp:** For 40 kWp: PV production covers a substantial share of the demand. In July, production (4651 kWh) exceeds demand (4006 kWh) by 645 kWh, indicating a high level of self-consumption.
- **50 and 60 kWp:** These scenarios cover a larger portion of the demand than the previous configurations but generate a substantial unwanted surplus during periods of low demand, mainly in summer, which is predominantly injected into the grid.

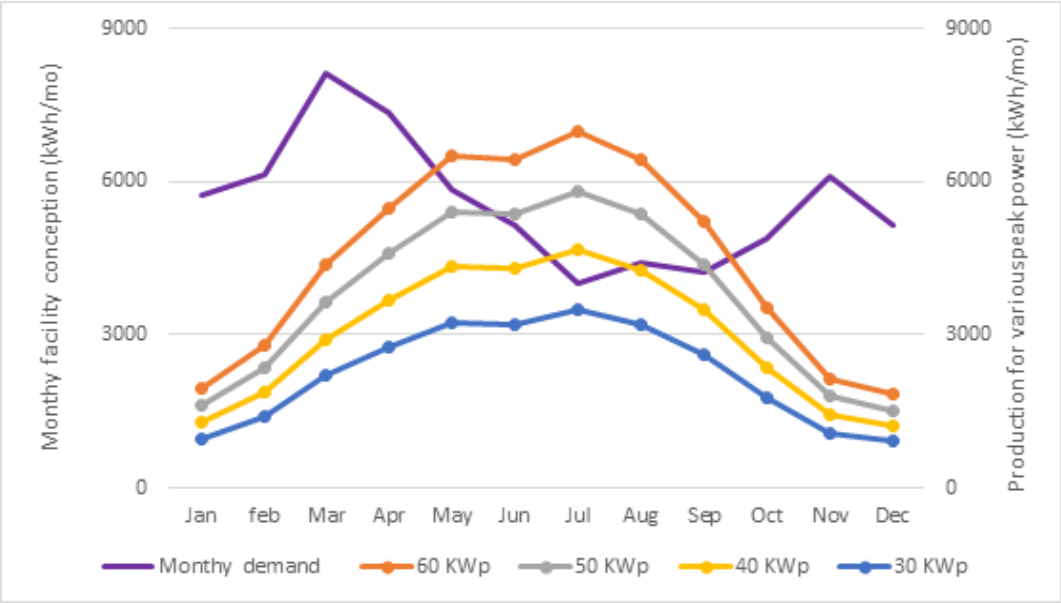

Fig 4. Monthly demand and simulated PV production for different peak power capacities.

The self-consumed PV energy and the surplus injected into the grid were quantified for each capacity scenario. Table 1 presents the monthly distribution of these energy flows as a function of the installed capacity. Increasing the installed capacity raises total production but also leads to higher surplus injections, particularly during the low-demand summer period. The site's load profile imposes a limit on the amount of energy that can be valorised locally; beyond this threshold, additional production does not result in a proportional improvement in self-consumption.

Table 1. Self-consumed and grid-exported energy (kWh/year) as a function of installed capacity.

Month	Self-consumption energy				Grid injection energy			
	60 KWp	50 KWp	40 KWp	30 KWp	60 KWp	50 KWp	40 KWp	30 KWp
Jan	1951	1626	1301	975	0	0	0	0
feb	2806	2338	1871	1403	0	0	0	0
Mar	4384	3653	2923	2192	0	0	0	0
Apr	5496	4580	3664	2748	0	0	0	0
May	5844	5411	4328	3246	649	0	0	0
Jun	5158	5158	4285	3214	1270	198	0	0
Jul	4006	4006	4006	3489	2971	1808	645	0
Aug	4426	4426	4281	3211	1996	926	0	0
Sep	4244	4244	3490	2617	990	118	0	0
Oct	3546	2955	2364	1773	0	0	0	0
Nov	2144	1787	1430	1072	0	0	0	0
Dec	1823	1520	1216	912	0	0	0	0
Total	45828	41703	35157	26852	7876	3050	645	0
Total/Demande	68%	62%	52%	40%	12%	5%	1%	0%

- 30 kWp: self-consumed energy represents 40% of demand, with no surplus injected. The generator is undersised relative to the load profile.

- 40 kWp: self-consumption reaches 52%, with marginal injection equivalent to 1% of demand, indicating a balanced match between generation and consumption.
- 50 kWp: the self-consumed share increases to 62%, while surplus injections reach 5%, indicating the emergence of structural surplus.
- 60 kWp: despite a maximum self-consumption of 68%, surplus injections rise to 12%.

An installed capacity of 40 kWp emerges as the optimal operating point, maximising the local utilisation of photovoltaic energy while minimising surplus injected into the grid. The LG425QAK-A6 PV module was selected for this study. Its nominal characteristics are presented in Table 2. To reflect the actual site conditions (temperature and irradiation), these parameters were corrected using the temperature coefficients provided by the manufacturer in Table 2.

Table 2. Electrical parameters of the LG425QAK-A6 module under standard test conditions.

P_{max}=425 W	I_{mpp} =10.31 A	V_{oc}=48.1 V	K_{Pmax} (T) =-0.29 %/°C
I_{sc} =10.84 A	V_{mpp}=41.3 V	K_{Isc} (T) = 0.04 %/°C	K_{Voc} (T) =-0.24 %/°C

The corrected PV module parameters are as follows:

- Open-circuit voltage (V_{oc}): 46.41 V at maximum module temperature of 60 °C and 51.33 V at minimum module temperature of −3 °C.
- Short-circuit curent (I_{sc}): 7.71 A.
- Voltage at the maximum power point (V_{mpp}): 39.85 V (at a maximum irradiation of 710.94 W/m²).

The system employs the Huawei SUN2000-40KTL-M3 inverter, selected for its high power density and multi-MPPT management capability. This device supports a maximum input voltage of 1100 V and provides an extended MPPT operating range between 200 V and 1000 V. With a current capacity of 26 A per MPPT, it ensures optimal compatibility with high-current modules and enables accurate maximum power point tracking under variable irradiation.

To achieve the target capacity of 40 kWp, a minimum of 94 LG425QAK-A6 modules is required. Design constraints impose series strings comprising between 5 and 21 panels, with a maximum of three parallel strings (Eq. 7 and Eq. 8).

To utilise the four available MPPTs (eight inputs in total), the final configuration was optimised to 96 panels. These panels are arranged into six groups of 16 modules, ensuring voltage balance. This distribution occupies both inputs of the first two MPPTs, while the remaining two MPPTs use one input each, leaving the unused inputs available for potential future expansions or optimisations. The spatial layout was calculated to avoid mutual shading between rows. With a solar altitude angle of 18° at the site, the minimum row spacing is 2.512 m, which is increased to 3 m to facilitate maintenance. The installation occupies a total area of 191 m², distributed evenly across three roof sections.

3.2 Simulation results and system performance

Figure 5 presents the monthly energy production normalised per kWp installed, distinguishing the final yield (Y_f), field collection losses (L_c) and system losses (L_s). The useful energy yield (Y_f) exhibits strong seasonal variability, with a maximum between May and July exceeding 5.4 kWh/kWp/day, and a minimum in winter ranging between 1.2 and 1.5 kWh/kWp/day. The annual average of Y_f is 3.45 kWh/kWp/day, which provides a robust estimate of the exploitable production available for the factory's electricity supply. Collection losses (L_c) remain stable at 0.36 kWh/kWp/day, mainly due to temperature

effects and DC cabling losses. System losses (L_s) are minimised at 0.06 kWh/kWp/day, confirming the high efficiency of AC conversion by the Huawei inverter. These results highlight the importance of matching PV generation for a 40 kWp capacity with the industrial load profile. The winter production decline suggests that grid imports are required to stabilise the site's energy balance.

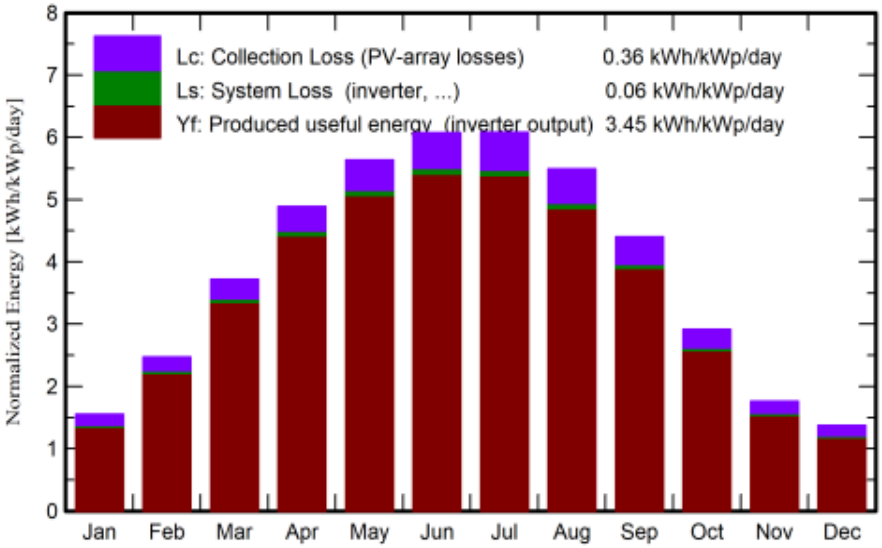

Fig 5. Normalised productions per installed kWp.

Table 3 presents the annual energy flows associated with the photovoltaic installation. The annual PV production is 49807 kWh, of which 25702 kWh are consumed directly on site, corresponding to a self-consumption rate of 51.6%, in agreement with the value obtained from the analytical calculation. The remaining production, 24105 kWh, is injected into the grid as surplus. The annual performance ratio (PR) is 87%, indicating satisfactory energy performance for the system, close to the values expected for well-sized industrial installations. Despite this significant PV contribution, the installation remains grid-dependent, with 41,486 kWh/year imported, mainly during the night when solar production is zero. Prior to PV integration, the entire electricity demand (67184 kWh/year) was supplied by the grid.

Table 3. PVsyst simulation results

Parameter	**Value**	**Parameter**	**Value**
Total annual energy produced (kWh/y)	49807	Energy used from the grid (kWh/y)	41486
Energy used from solar (kWh/y)	25702	Total energy consumed (kWh/y)	67184
Energy sent to the grid (kWh/y)	24105	Performance Ratio (%)	87

3.3 Economic assessment

Table 4 summarises the main cost items associated with the photovoltaic installation. The total investment cost (CAPEX) is estimated at €45360. The estimate includes the main expenditure items required for the system implementation. Photovoltaic modules represent the largest share of the budget, with 96 units priced at €300 each. The inverter is valued at €4356 for a single unit. Other cost items include the supporting structure, sized to accommodate all modules, with 96 units at €35 each; cabling, estimated at 200 m with a unit cost of €3/m; and labour, accounted for as a lump-sum estimate.

The annual economic assessment distinguishes between self-consumed energy, surplus energy sold to the grid, and energy purchased from the grid. Table 5 presents the detailed calculations associated with this valuation. The selling price of surplus energy is set at €0.05/kWh. The purchase price varies

according to demand, with a daytime tariff of €0.20/kWh and a night-time tariff of €0.25/kWh. In the absence of detailed hourly data for the pre-installation period, a weighted average tariff of €0.23/kWh is adopted to estimate the baseline annual cost. This tariff provides a simplified representation of the day/night structure and ensures a consistent comparison with the post-installation situation.

Table 4. Photovoltaic installation costs

Component	**Unit Price (€)**	**Quantity**	**Total Price (€)**
Panels	250	96	24000
Inverter	4000	1	4000
Mounting structure	35	96	3360
Cabling (estimated)	–	–	2500
Labor (estimated)	–	–	9000
Other (protections, monitoring, etc.)	–	–	2500
Total CAPEX	–	–	45360

Table 5. Annual economic balance of the photovoltaic installation

Energy kWh/year	Quantity(kWh/y)	U. Price(€/KWh)	Price (€/y)
Annual PV energy produced	49807	–	–
PV energy produced consumed	25702	0.20	5140
PV Energy sent to the grid (surplus)	24105	0.05	1205
Energy used from the grid: purchased (night tariff)	41486	0.25	10371
Total energy consumption before PV installation	67184	0.23	15452

Self-consumed PV energy corresponds to an annual saving of €5140.4. The surplus injected into the grid generates annual revenue of €1205.3. The cost of energy purchased from the grid amounts to €10371.5 per year. Before installation, the annual electricity bill is estimated at €15452.3. After PV integration, the electricity bill equals the grid purchase cost (€10371.5) minus the surplus sale revenue (€1205.3), resulting in €9166.2. The annual bill reduction is €6286.1, corresponding to a decrease of approximately 41%. The CAPEX is estimated at €45360. Operation and maintenance costs (OPEX) are set at 1.5% of CAPEX, i.e., €680 per year, which is consistent with sector references for PV installations without storage. The annual gains derived from the energy balance amount to €6286.1. The net annual gain is obtained by subtracting OPEX from this amount, resulting in a net gain of €5606.1 per year. Figure 6 illustrates the cumulative net gain over time. The cumulative net gains exceed the CAPEX from the 8th year onwards, corresponding to a payback period of approximately 8 years. Local electricity tariffs can significantly influence the selection of the optimal PV capacity. Higher electricity prices may justify larger system sizes by increasing savings from self-consumption, whereas lower tariffs could reduce the economically optimal capacity.

3.4 Environmental impact assessment

The 40 kWp PV system yields an annual CO_2 emission avoidance of 14.73 $tCO_2\ yr^{-1}$. Considering the total embodied carbon footprint of the system, estimated at 71.9 tCO_2 by PVsyst, the Carbon Payback Time (CPBT) is reached in 4.88 years. This period represents less than 20% of the system's 25-year lifetime, indicating that over 80% of the operational phase provides a net carbon benefit.

Figure 7 illustrates the dynamic evolution of the cumulative CO_2 emission balance over the system's lifespan. The simulated curve crosses the zero line at the beginning of the fifth year, confirming the calculated CPBT. After 25 years of operation, and accounting for progressive module degradation and

various system losses, the final net avoided emission reaches 255.6 tCO_2 . This substantial positive balance demonstrates the effectiveness of the PV installation as a highly relevant decarbonization strategy for the industrial site.

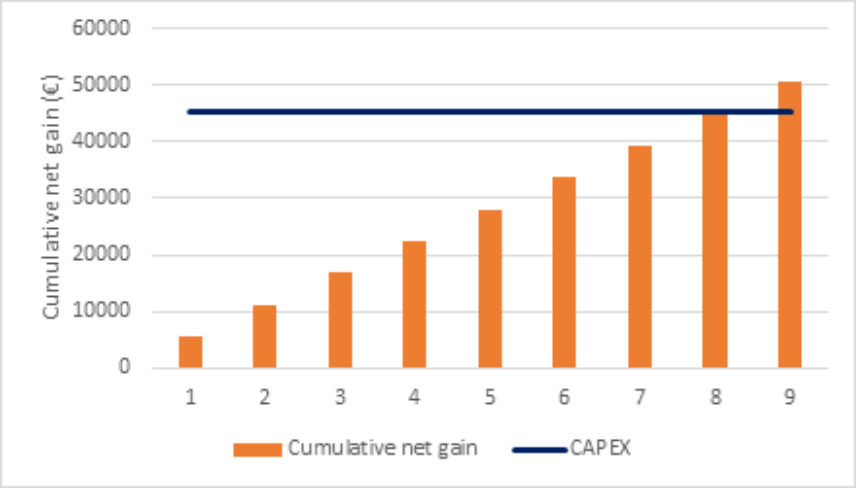

Fig 6. Cumulative net gain and investment cost (CAPEX) of the PV system.

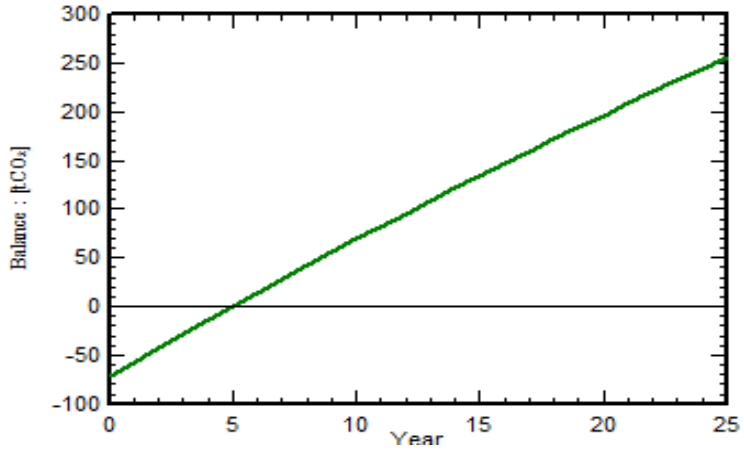

Fig 7. Evolution of the cumulative CO_2 emission avoidance for the PV installation.

3.5 Multi-criteria analysis and optimal system configuration

The 40 kWp PV system demonstrates superior technical performance compared to the 30, 50, and 60 kWp scenarios. To enable a multi-criteria comparison, the technical, economic, and environmental performance of all scenarios was evaluated. The simulations were conducted using PVsyst under the same assumptions applied to the 40 kWp case, including the factory load profile, climatic data, and PV module. For each capacity, the system design was adjusted in terms of inverter selection, number of modules, and PV field layout: 30 kWp with 72 modules and a SUN2000-30KTL-M3 inverter; 50 kWp with 120 modules and a SUN2000-50KTL-M3 inverter; and 60 kWp with 140 modules and a SUN2000-60KTL-M0 inverter. Table 6 summarises the main outputs.

Table 7, summarises the indicators calculated for each configuration. The solar fraction increases progressively with installed power, from 33.92 % for 30 kWp to 46.10 % for 60 kWp. The specific gain reaches a maximum at 30 kWp (173 €/kWp/year) and then decreases with oversizing. The 40 kWp and 50 kWp scenarios achieve the highest specific CO_2 avoided, with 0.36 tCO_2 /kWp/year.

Table 6. Technical, economic, and environmental variables for the four PV power levels

Installed Power (kWp)	**30**	**40**	**50**	**60**
Technical				
Annual PV generation (kWh/year)	35892	49807	62749	69743
PV self-consumed energy (kWh/year)	22786	25702	32900	38769
Surplus injected to the grid (kWh/year)	13106	24105	29849	30974
Imported energy from the grid (kWh/year)	44398	41486	37335	36210
Economic				
Investment cost (CAPEX €)	38520	45360	52200	60900
Savings from self-consumption (€/year)	4557	5140	6580	7753
Revenues from surplus injection (€/year)	655	1205	1492	1548
Payback period (years)	8.31	8.00	7.16	7.26
Environmental				
CO_2 emissions avoided (tCO_2 /year)	10.3	14.73	18	20
Carbon payback time (years)	8.7	5	5	4.5

Table 7. Indicator values for the PV configurations

Installed Power (kWp)	30	40	50	60
Technical: Solar Fraction FR (%)	33.92	38.3	44.83	46.1
Economic: Specific Gain (€/kWp/year)	173	158	161	155
Environmental: Specific CO_2 Avoided (tCO_2 /kWp/year)	0.34	0.36	0.36	0.33

Normalising the indicators by their respective maximum values allows them to be represented graphically on a common scale of [0, 1]. Figure 8 presents the comparative radar chart of the four scenarios, integrating the three pillars: technical, economic, and environmental, represented by their corresponding normalised indicators.

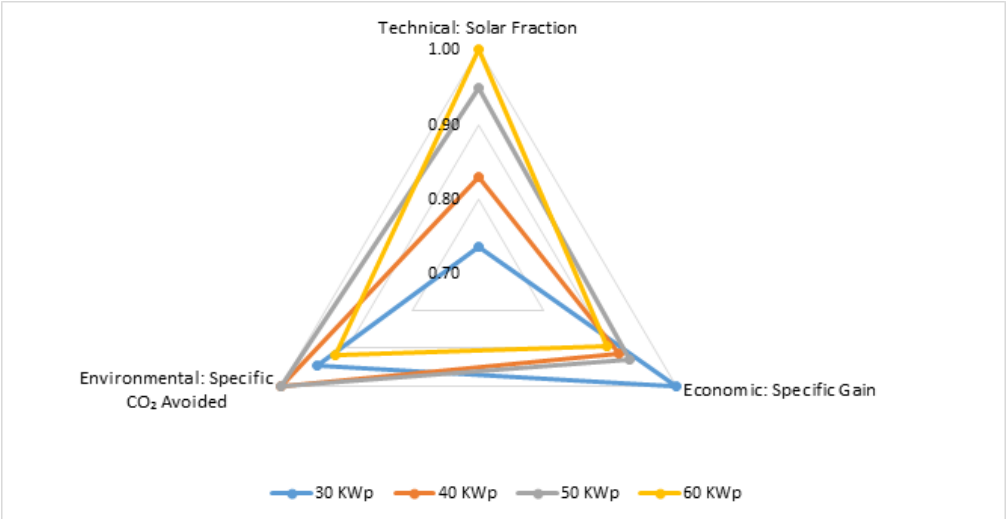

Fig 8. Comparative radar chart of the PV configurations

The 30 kWp configuration, although exhibiting the maximum specific gain (1.00), remains limited by a normalised solar fraction of 0.74. This indicates under-sizing, which is insufficient to meet industrial demand and the goal of energy self-consumption effectively. In contrast, the 60 kWp configuration

achieves the maximum normalised solar fraction (1.00). However, it produces a high annual surplus of 30974 kWh, representing 44 % of total production. This oversizing reduces efficiency in an industrial self-consumption context and results in a significant CAPEX.

The 40 kWp and 50 kWp configurations exhibit a balanced performance across the economic and environmental pillars. The 50 kWp system achieves a slightly higher normalised solar fraction, reaching 0.97 compared to 0.83 for the 40 kWp configuration. However, it produces an annual surplus that exceeds that of the 40 kWp system by 5744 kWh, representing an increase of +23.8 %. Its capital expenditure is also €6840 higher, corresponding to a +15 % increase. These additional costs and surplus generation reduce overall efficiency and profitability in an industrial self-consumption context.

The multi-criteria analysis, illustrated by the radar chart, identifies the 40 kWp configuration as the most balanced option across the technical, economic, and environmental pillars. It achieves a payback period of eight years and a carbon payback time of 5.00 years, confirming both financial viability and environmental effectiveness. Based on this overall balance, limited surplus generation, and economic rationality, the 40 kWp system is selected as the optimal configuration. It aligns electricity production with demand, maximizes carbon mitigation per unit installed, and maintains a moderate initial investment.

4. CONCLUSION

This study evaluated the technical, economic, and environmental performance of rooftop photovoltaic systems for industrial self-consumption, with surplus electricity exported to the grid. Four capacities (30, 40, 50, and 60 kWp) were simulated using PVsyst, considering the factory load profile, roof geometry, and corrected solar irradiation (13° azimuth, 6° tilt).

The 30 kWp system was under-sized, meeting only 33.9 % of annual demand. The 60 kWp system achieved the highest solar fraction with 46.1 % but generated an excessive surplus of 30974 kWh, representing 44 % of total production, indicating oversizing. The 40 kWp and 50 kWp systems provided a more balanced match between generation and on-site consumption.

The 50 kWp system increased annual energy generation by approximately 26 % compared to the 40 kWp, but it also produced an undesirable 23.8 % surplus and required 15 % higher CAPEX, reducing overall economic efficiency. In contrast, the 40 kWp system achieved a net payback period of 8 years, ensuring financial viability with moderate investment.

Both the 40 kWp and 50 kWp configurations maximised CO_2 savings (0.36 tCO_2 /kWp/year). The 40 kWp system reached carbon payback in 5 years and avoided a cumulative 285.6 tCO_2 over a 25-year lifespan, demonstrating significant and sustained environmental benefits.

Multi-criteria analysis integrating technical, economic, and environmental indicators confirmed that the 40 kWp system represents the optimal configuration. It balances generation with consumption, limits surplus injection, maximizes environmental gains, and ensures economic rationality. Further improvements could incorporate dynamic electricity tariffs and active load management to enhance self-consumption and surplus utilisation in industrial PV systems.

Future work will involve on-site experimental implementation and real-time monitoring to validate the findings under actual operating conditions.

REFERENCES

Al Shumrani MA, Gulistan M, Abbas T. (2026) Multi-criteria decision making approach for solar energy implementation using N-cubic fuzzy interaction aggregation operators. Scientific Reports, 16, 1138. doi:10.1038/s41598-025-30869-7.

Başaran K, Özdemir MT, Bayrak G. (2025). Sizing and techno-economic analysis of utility-scale PV systems with energy storage systems in factory buildings: An application study. Applied Sciences, 15(7), 3876. Doi: 10.3390/app15073876.

Belhaouas N, Hafdaoui H, Mehareb F. (2025). Analysis of the relationship between photovoltaic temperature coefficients and varying solar irradiance levels. Journal of Renewable Energies, SIEER'2025 (Special Issue), 28(5), 103–111. Doi: 10.54966/jreen.v28i5.1548.

Bouroumeid Y, Jbilou M, Bechekir SE, Arezki M, Ghaitaoui EA, Oulad Naou BEK, Taghezouit B, Assem H, Madjoudj N, Chahtou A, Saheb-Koussa D. (2024). Analysis of the efficiency of a solar photovoltaic power plant linked to the electrical grid. Journal of Renewable Energies, IREnDAYS'24 (Special issue), 67–73. Doi: 10.54966/jreen.v1i1.1236.

Camilo FM, Castro R, Almeida ME, Fernão Pires V. (2017). Economic assessment of residential PV systems with self-consumption and storage in Portugal. Solar Energy, 150, 353–362. Doi: 10.1016/j.solener.2017.04.062.

Chen Jong F., Mohamud Ahmed M. (2024). Multi criteria decision making solutions for optimal solar energy sites identification: A systematic review. IEEE Access, 12, 143458-143484, 2024, doi: 10.1109/ACCESS.2024.3461948.

Ciocia, A., Amato, A., Di Leo, P., Fichera, S., Malgaroli, G., Spertino, F., & Tzanova, S. (2021). Self-consumption and self-sufficiency in photovoltaic systems: Effect of grid limitation and storage installation. Energies, 14(6), 1591. Doi: 10.3390/en14061591.

García JL, Perdigones A, Benavente RM, Álvarez J, Baptista F, Mazarrón FR. (2023). Feasibility of photovoltaic systems for the agrifood industry in the new energy and climate change context. Agronomy, 13(10), 2620. Doi : 10.3390/agronomy13102620.

Hazem T, Cheghib H, Fezzani A, et al. (2025). Performance evaluation of grid connected photovoltaic pilot plant in Saharan climate using experimental and numerical analysis. Scientific Reports, 15, 32488. Doi: 10.1038/s41598-025-19300-3.

Hu X, Hu J, Zhang H. (2020). A life-cycle cost-benefit analysis for rooftop photovoltaic systems in lightweight steel-structured industrial buildings. Environmental Science & Sustainable Development, 5(2), 20–31. Doi: 10.21625/essd.v5i2.757.

Jäger Waldau A. (2025). Snapshot of photovoltaics. EPJ Photovoltaics, 16, 22. Doi: 10.1051/epjpv/2025012.

Kalogirou S A. (2017). McEvoy's handbook of photovoltaics: Fundamentals and applications. 3rd ed. Oxford: Elsevier.

Laksono DT, Laksono DT, Fahmi MF, Afrianti R, Dodi N. (2025). Technical performance analysis of a 1 MWp grid-connected photovoltaic system in Pangkalan Kerinci, Indonesia using PVsyst simulation. International Journal of Science, Engineering, and Information Technology, 10(01). https://journal.trunojoyo.ac.id/ijseit/article/download/32479/pdf.

Mohand Kaci G, Mahrane A, Ghedamsi K, Chikh M. (2024). Techno-economic feasibility analysis of grid-connected residential PV systems in Algeria. Energy & Environment, 35(4), 1936–1966. Doi : 10.1177/0958305X221146953.

Neumüller, A., Geier, S., & Österreicher, D. (2023). Life Cycle Assessment for Photovoltaic Structures-Comparative Study of Rooftop and Free-Field PV Applications. Sustainability, 15, 13692. Doi: 10.3390/su151813692.

Pedrero J, Hernández P, Martínez Á. (2021). Economic evaluation of PV installations for self-consumption in industrial parks. Energies, 14(3), 728. Doi: 10.3390/en14030728.

Rouabhia A, Dabou R, Abderrahmane A, Ziane A, Bouraiou A, Khelifi S, Sahouane N, Necaibia A, Blal M. (2025). Low-cost real-time monitoring for enhanced efficiency in PV systems. Journal of Renewable Energies, 28(1), 81–92. Doi: 10.54966/jreen.v28i1.1348.

Rus, T., Moldovan, R.-P., & Pardo Picazo, M. Á. (2024). LCA analysis of a roof-mounted PV system: A Romanian case study. Frontiers in Environmental Science, 12, 1413629. Doi: 10.3389/fenvs.2024.1413629.

Sánchez-Jiménez JL, Jiménez-Castillo G, Rus-Casas C, Martínez-Calahorro AJ, Muñoz-Rodriguez FJ. (2025). Performance evaluation of photovoltaic self-consumption systems on industrial rooftops under continental Mediterranean climate conditions with multi-string inverter topology. Energy Reports, 14, 1020–1042. Doi: 10.1016/j.egyr.2025.06.047.

Yıldırım B, Düzkaya H. (2025). Comparative analysis with PVGIS and PVsyst for solar energy production in Bahşılı region of Kırıkkale. Gazi Üniversitesi Fen Bilimleri Dergisi Part C: Tasarım ve Teknoloji, 13(3), 877–891. Doi : 10.29109/gujsc.1661431.

Zaghba L, Khennane Benbitour M, Fezzani A, Mekhilef S, Borni A. (2025). Comprehensive performance assessment of two grid-tied photovoltaic systems in a hot arid climate: A three-year theoretical and experimental analysis. Renewable and Sustainable Energy Reviews, 216, 115643. Doi: 10.1016/j.rser.2025.115643.

Web sites

Google LLC. Google Earth Pro (Version 7.3), https://earth.google.com/; [accessed 29 April 2025].

IEA. (2025). Global energy review 2025. Source: IEA, International Energy Agency. https://www.iea.org; 2025 [accessed 03 January 2026].

MeteoGalicia. Meteorological and climate data portal, https://www.meteogalicia.gal; [accessed 29 April 2025].

PVGIS - Photovoltaic Geographical Information System, https://ec.europa.eu/jrc/en/pvgis; [accessed 13 April 2025].

SunCalc - Sun position calculator, https://suncalc.org; [accessed 29 April 2025].